Nanoscale

PAPER

View Article Online
View Journal | View Issue

Cite this: *Nanoscale*, 2023, **15**, 5865

Microfluidic production of nanogels as alternative triple transfection reagents for the manufacture of adeno-associated virus vectors

Zoe Whiteley,[a] Giulia Massaro,[b] Georgios Gkogkos,[c] Asterios Gavriilidis,[c] Simon N. Waddington,[d,e] Ahad A. Rahim[b] and Duncan Q. M. Craig *[a]

Received 15th November 2022,
Accepted 25th February 2023

DOI: 10.1039/d2nr06401d

rsc.li/nanoscale

Adeno-associated viral vectors (AAVs) have proved a mainstay in gene therapy, owing to their remarkable transduction efficiency and safety profile. Their production, however, remains challenging in terms of yield, the cost-effectiveness of manufacturing procedures and large-scale production. In this work, we present nanogels produced by microfluidics as a novel alternative to standard transfection reagents such as polyethylenimine-MAX (PEI-MAX) for the production of AAV vectors with comparable yields. Nanogels were formed at pDNA weight ratios of 1 : 1 : 2 and 1 : 1 : 3, of pAAV *cis*-plasmid, pDG9 capsid *trans*-plasmid and pHGTI helper plasmid respectively, where vector yields at a small scale showed no significant difference to those of PEI-MAX. Weight ratios of 1 : 1 : 2 showed overall higher titers than 1 : 1 : 3, where nanogels with nitrogen/phosphate ratios of 5 and 10 produced yields of $\approx 8.8 \times 10^8$ vg mL^{-1} and $\approx 8.1 \times 10^8$ vg mL^{-1} respectively compared to $\approx 1.1 \times 10^9$ vg mL^{-1} for PEI-MAX. In larger scale production, optimised nanogels produced AAV at a titer of $\approx 7.4 \times 10^{11}$ vg mL^{-1}, showing no statistical difference from that of PEI-MAX at $\approx 1.2 \times 10^{12}$ vg mL^{-1}, indicating that equivalent titers can be achieved with easy-to-implement microfluidic technology at comparably lower costs than traditional reagents.

1 Introduction

Gene therapy offers a transformative approach to the treatment of many diseases, particularly those for which poor or no treatment options were previously available. Adeno-associated viral vectors (AAVs) represent one of the most widely studied gene delivery systems, comprising recombinant viruses based on the naturally occurring AAV serotype 2 (AAV2), itself composed of a single-stranded DNA genome of approximately 4.7 kb.[1] AAVs have shown considerable success in two recently approved products; Luxturna (voretigene-neparvovec-rzyl), an AAV2-based gene therapy for the treatment of inherited retinal disease in 2017 [2–4] and Zolgensma (onasemnogene abeparvovec) utilising an AAV9 vector for the treatment of spinal muscular atrophy.[5] The marked success of AAV vectors can be attributed to their ability to efficiently transfect a broad range of cell types, promote long-term gene expression and exhibit low pathogenicity.[1,6]

The clinical capabilities of AAV vectors have prevailed in spite of difficulties experienced in their manufacture. AAV preparation is a multi-step procedure, consisting of plasmid production, cell expansion, transfection of typically three plasmids, vector production and finally purification.[7] While vector manufacturing in non-GMP settings within academic labs is generally reproducible and cost-effective, the process at a larger scale and at GMP is considerably more challenging and expensive. AAV vectors can be produced by several methods, including triple transfection where three plasmids are introduced in to producer cells (outlined in more detail below), adenovirus acting as a helper virus[8] and insect cells using baculovirus expression systems.[9] Shortcomings of triple transfection include inefficient transfection efficiency and high costs of DNA and reagents.[7,10] The three plasmids are typically; an AAV *trans*-plasmid encoding replication (*Rep*) and capsid (*Cap*) genes, an AAV *cis*-plasmid coding for the gene of interest, promotor and inverse terminal repeats (ITRs) and a third plasmid encoding the adenovirus helper genes E4, E2a and VA.[11,12] The transfection of producer cells for AAV manufacture necessitates a transfection reagent, usually polyethylenimine (PEI), calcium phosphate or cationic liposomes such as lipofectamine.[13–15]

[a]*Department of Pharmaceutics, UCL School of Pharmacy, University College London, 29-39 Brunswick Square, London, WC1N 1AX, UK. E-mail: duncan.craig@ucl.ac.uk*
[b]*Department of Pharmacology, UCL School of Pharmacy, University College London, 29-39 Brunswick Square, London, WC1N 1AX, UK*
[c]*Department of Chemical Engineering, University College London, Torrington Place, London, WC1E 7JE, UK*
[d]*Institute for Women's Health, University College London, 84-84 Chenies Mews, London, WC1E 6HU, UK*
[e]*MRC Antiviral Gene Therapy Research Unit, Faculty of Health Sciences, University of the Witswatersrand, Johannesburg, South Africa*

Often considered the most cost-effective transfection method, manufacture using calcium phosphate is difficult to scale up and batch-to-batch variations can negatively impact the vector titer,[13] where it was reported that sub-standard preparation could result in over a 10-fold decrease in the production of AAV.[16] Lipofectamine offers high transfection efficiencies, though its use is limited by the considerable costs of reagents for large-scale transfections[16] and in some cases high cytotoxicity.[17] Since the first reporting of complexing PEI with nucleic acids,[18] this approach has been widely used in triple transfection for AAVs,[14,19–22] owing to the ease of preparation and reduced cost in comparison to cationic liposomes. Triple transfection with PEI still requires optimisation given its inability to withstand pH changes, high cytotoxicity to producing cell lines[7] and the opportunity for batch-batch variations. In recent years, novel transfection reagents such as FectoVIR-AAV,[23] PEI-Max[24] and PEI-Pro[25] have been developed and used in both small and large-scale manufacturing, though the expense of these reagents may limit their use.

Recent research focusing on improvements in transfection has relied on the optimisation of PEI/pDNA vectors, in terms of their total pDNA content and the ratio between constituent plasmids. Huang *et al.* produced PEI : pDNA complexes for transfection with optimised pDNA ratios, which resulted in an overall decrease in the pDNA content without compromising AAV2 vector quantity, thus resulting in lower costs of reagents.[19] A nitrogen/phosphate (NP) ratio of 40 was maintained throughout the study, where the highest titer was seen at 10^{12} vg mL^{-1}.[19] The plasmid DNA ratios between the three plasmids may also impact the transfection efficiency and vector titer, hence Zhao *et al.* varied the ratios of pHelper : pRC : pAAV, using plasmid ratios of commonly used 2 : 1 : 1 respectively and their optimised ratio of 1 : 5 : 0.31.[26] Although insignificant differences in vector yields on HEK293 adherent cells were found, the 5.1-fold reduction in the quantity of pAAV DNA used in the optimised ratio may, depending on the gene of interest, reduce the plasmid toxicity to production cells.[26,27] Most recently, Guan *et al.* optimised various aspects of production including, the type of reagent for transfection in order to achieve a scalable process with high yields.[28] Guan *et al.* compared calcium, lipofectamine and cationic liposomes, formulated in-house, as transfection reagents on adherent HEK293AAV cells, generating AAV-DJ/8 titers of 3.87×10^9 gc mL^{-1}, 8.37×10^8 gc mL^{-1} and 5.29×10^8 gc mL^{-1} respectively. Although the cationic liposomes synthesised in-house showed lower transfection than calcium phosphate and lipofectamine, it was argued that their use could significantly reduce the cost of AAV manufacture.[28]

The previously discussed methods require the manual mixing of pDNA and the relevant transfection agent, hence differences in preparation between operators may lead to high batch variations[13] and thus inconsistent transfection efficiencies. In this work, we propose nanogels as novel transfection reagents for the manufacture of AAV9 vectors, fabricated by microfluidics to surmount the obstacles of batch-produced transfection reagents. Nanogels are dispersions of hydrogel nanoparticles, with a cross-linked polymeric core.[29,30] They have been previously investigated for their use as gene delivery vehicles,[31–34] given their preparation under mild conditions, rendering them suitable for the encapsulation of biological macromolecules.[35] Ionic gelation is the classical method of producing nanogels, relying on the presence of polyelectrolytes to form physical cross-links,[36] similar in nature to the complexation of positively charged PEI with negatively charged pDNA. Batch-to-batch variations may also impede the production of nanogels, as several variables can affect their formulation such as weight ratio, temperature, pH and concentration of polymer and cross-linker.[37] Microfluidics, which refers to the control and manipulation of fluid flow at a microscopic scale, is used in this work to formulate nanogels and overcome such issues. This method of production offers a continuous process, alleviates batch variation and aids the production of monodispersed particles through fine control of process parameters.[38] An overview of the triple transfection process in this study is demonstrated in Fig. 1.

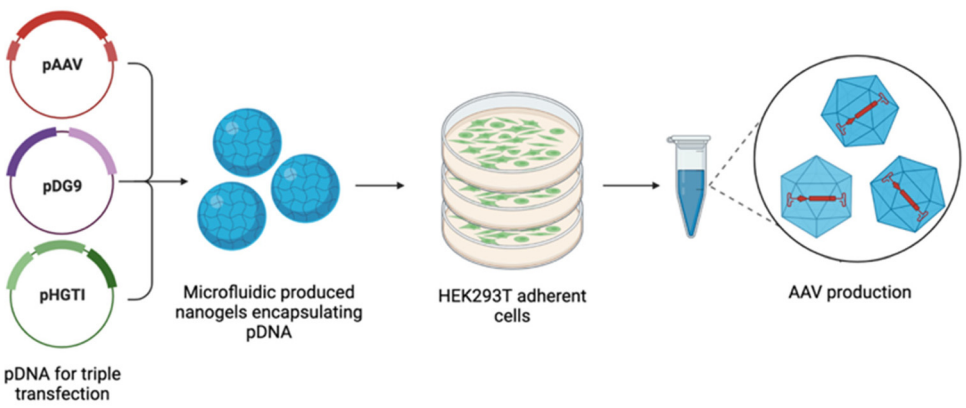

Fig. 1 Schematic of the triple transfection process using microfluidics produced nanogels for the encapsulation of the *cis*-plasmid pAAV, the *trans*-plasmid pDG9 and the helper plasmid pHGTI and transfection of adherent HEK293T cells. Adapted from "Plasmid Transfection Workflow" for the combination of three plasmids in PEI nanoparticles by BioRender.com (2022). Retrieved from https://app.biorender.com/biorender-templates.

The microfluidic system designed in this study builds on previous research conducted on the microfluidic production of nanogels and polymeric nanoparticles, which largely focussed on using T-shaped microchips fabricated from polydimethylsiloxane (PDMS).[39,40] Glass reactors are anticipated to be better-suited to this manufacturing process as they are easy to clean and able to prevent fouling of polymers on the channel walls,[41] a key requirement of equipment used in the manufacture of clinical grade AAV.[42] A glass coaxial flow reactor (CFR), shown in Fig. 2, was fabricated in this work, further developed from Whiteley *et al.*[41] The reactor operated under laminar flow, which is typically characterised by layers of fluid flowing in parallel to one another, mixing only by diffusion. This flow regime is used in the production of the transfection reagent with the intent of imparting little shear stress onto the three plasmids used, thus reducing the incidence of damage and degradation. In an effort to reduce the cytotoxicity and enhance the transfection efficiency of PEI, a polymer conjugate of carboxymethyl chitosan (CMC) and branched PEI (bPEI) is used in this study.[43] CMC, a derivative of chitosan, was selected to conjugate to PEI due to its low toxicity, biocompatibility and ability to form gels.[44]

In this work, we present an alternative triple transfection method for AAV9 production, using nanogels produced by microfluidics to encapsulate the pDNA, compared to the widely used PEI-MAX polyplexes as a control. To the best of our knowledge, nanogels have not yet been implemented as triple transfection reagents, however, they offer high encapsulation of biomaterials, biocompatibility and low toxicity in comparison to other commercially available reagents. We propose that the CFR will allow a controlled and reproducible method for the manufacture of nanogels as triple transfection reagents and hence facilitate the synthesis to become a continuous process with high yields and rapid production.

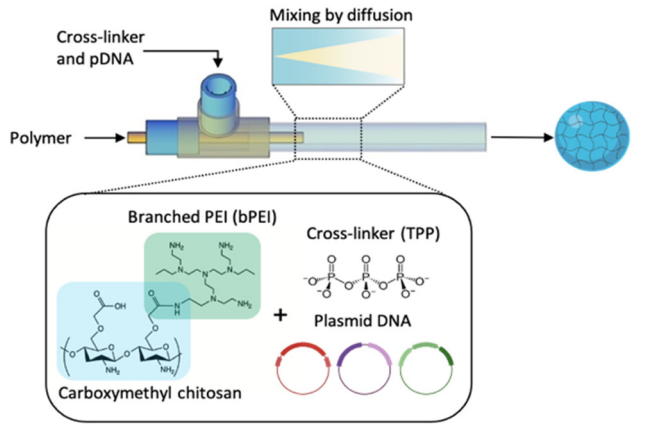

Fig. 2 Schematic of CFR demonstrating the smaller glass microcapillary delivering the carboxymethyl chitosan and branched PEI (CMC–bPEI) polymeric solution and the pAAV, pDG9 and PHGTI plasmids in solution with sodium tripolyphosphate as the cross-linker through the outer stream. The solutions mix by diffusion to form nanogels by ionic gelation.

2 Materials and methods

2.1 CMC–bPEI polymer production

Carboxymethyl chitosan (CMC) 210–300 kDa (medium molecular weight) (Chem Cruz Biochemicals, Texas, USA) and branched PEI (bPEI) at 25 kDa (Sigma Aldrich, Gillingham, UK) were conjugated using a 1-ethyl-3-(3-dimethylaminopropyl)carbodiimide hydrochloride (EDC) (Thermo Fisher Scientific, UK) and *N*-hydroxysuccinimide (NHS) (Thermo Fisher Scientific, UK) conjugation protocol adapted from Park *et al.*[43] Solutions of 0.7% (w/v) CMC and 30% (w/v) bPEI were prepared in distilled water and mixed in equal parts to a total volume of 30 mL. This solution was allowed to mix at room temperature for 30 minutes before the pH was adjusted to 5.5 with 1 M HCl. An aqueous solution of EDC (192 mg) and NHS (115 mg) in 10 mL was prepared, creating a molar ratio of 1 : 2 respectively and added dropwise to the adjusted CMC–bPEI mixture under stirring for 24 hours. The resulting solution was dialysed against PBS for 48 hours using a 7000 molecular weight cut-off (MWCO) snakeskin dialysis membrane (Thermo Fisher Scientific, UK) to remove the reaction waste products, with a suspending solution medium change after 24 hours. The polymer remaining in the dialysis membrane was freeze-dried and stored at −20 °C.

2.2 Fabrication of microfluidic coaxial flow reactor

The CFR design has been previously discussed and adapted from Whiteley *et al.*[41] An inner glass microneedle with an internal diameter (ID) of 0.2 mm and length of 32 mm (Drummond Scientific, PA, USA) was fixed using a PEEK T-junction with a 0.020″ thru-hole diameter and 1/16″ outer diameter (OD) (Cole Parmer, Saint Neots, UK) inside a larger glass tube of ID 1.6 mm, an OD of 3 mm and length 162 mm (VWR International, Lutterworth, UK), creating a 3D flow-focussing profile whereby the core solution is fully surrounded by the sheath solution. The polymer solution of CMC–bPEI at varying concentrations according to the NP ratio, was used as the core solution and TPP mixed in solution with the 3 plasmids; pAAV, pDG9 and pHGT1, at a fixed concentration discussed below, was used as the outer sheath solution.

2.3 Preparation of nanogels in CFR

Nanogels were produced at a variety of NP ratios, where the number of moles of the phosphate in the pDNA and sodium tripolyphosphate (TPP) (Sigma Aldrich, UK) cross-linker remained consistent throughout all experiments and the number of moles of nitrogen from CMC–bPEI polymer was varied to achieve the desired ratio. The anionic components of the formulation were first mixed together outside of the reactor, where a solution of 0.01% (w/v) TPP was mixed with the pDNA by light vortexing for 2–3 seconds. To achieve a pDNA weight ratio of 1 : 1 : 2, 13.125 μg of pAAV was added per 2.5 mL nanogel formulation, 13.125 μg/2.5 mL of pDG9 and 26.25 μg/2.5 mL of pHGTI. For a pDNA weight ratio of 1 : 1 : 3, 10.5 μg/2.5 mL of pAAV and pDG9 were mixed with 31.5 μg/2.5 mL of pHGTI. The resulting TPP-pDNA solution was used

as the sheath stream of the CFR in the outer glass tube (Fig. 2).

The CMC–bPEI was used at concentrations of; 0.0048% (w/v) (NP1), 0.024% (w/v) (NP5), 0.048% (w/v) (NP10), 0.072% (w/v) (NP15), 0.096% (w/v) (NP20) and 0.120% (w/v) (NP25). As this solution behaves as the cationic component of the nanogel, it is delivered through the core stream in the smaller glass microneedle of the CFR. The core stream flow rate is set to 80 μL min^{-1} and the sheath stream to 800 μL min^{-1}, creating a flow ratio (core flow rate/sheath flow rate) of 0.1, achieving an overall production rate of 0.88 mL min^{-1} of nanogels in the CFR.

2.4 Preparation of PEI-MAX transfection mix

For the small-scale transfections carried out in 6-well plates, PEI-MAX (Polysciences, Inc. Warrington, PA, USA) and pDNA polyplexes at pDNA weight ratios of both 1 : 1 : 2 and 1 : 1 : 3 were used. The total quantity of pDNA added for the transfection remained constant at 2.5 μg per well, irrespective of the weight ratio of pDNA used in the formulations. Hence, for 1 : 1 : 2 ratios the mixture of pDNA contained; 0.625 μg per well of pAAV, 0.625 μg per well of pDG9 and 1.25 μg per well of PHGTI and for 1 : 1 : 3 ratios the mixture contained; 0.5 μg per well of pAAV, 0.5 μg per well of pDG9 and 1.5 μg per well. Following a PEI : pDNA respective weight ratio of 2.25 μg : 1 μg, 2.8 μL of 2 mg mL^{-1} PEI-MAX was added to the pDNA mixture and allowed to complex for 10–15 minutes at room temperature prior to transfection.

For the 10-dish large-scale transfections, only PEI-MAX/pDNA polyplexes at weight ratios of 1 : 1 : 2 were used for AAV production, at a total pDNA quantity of 52.5 μg pDNA per dish, adapted from the protocol of Hughes *et al.*[45] To prepare this ratio, pAAV at 13.125 μg per dish was mixed with 13.125 μg per dish of pDG9 and 26.25 μg per dish of pHGTI in a final volume of 2.5 mL Opti-MEM per dish. To achieve a final weight ratio of 2.25 μg : 1 μg of PEI : DNA, 59 μL of 2 mg mL^{-1} PEI-MAX was added to the pDNA mixture and allowed to complex for 10–15 minutes.

2.5 Cell preparation

HEK293T AAVPro cells were obtained from Takeda Bio (Japan) from human sources. The cells were grown in Dulbecco's modified Eagle's medium (DMEM) growth medium with high glucose and GlutaMAX, supplemented with 10% (v/v) heat-deactivated fetal bovine serum (FBS) and 1% (v/v) penicillin/streptomycin (all products purchased from Gibco, Massachusetts, USA) at 37 °C and 5% CO_2. For small-scale transfections, cells were seeded at 0.25×10^6 cells per well in 2 mL DMEM GlutaMAX media and for large-scale transfections in 150 cm^2 cell culture dishes (Thermo Fisher Scientific, UK), cells were seeded at a density of 1.3×10^7 per dish to a final volume of 20 mL media per dish.

2.6 Transfections

Once 70–80% confluency was achieved, HEK293T cells were triple transfected with both PEI-MAX polyplexes and nanogel formulations at varying NP ratios and pDNA weight ratios, at both small (6-well plates) and large scale (10-dishes). At the time of transfection in 6-well plates, 2.5 μg per well (48 μL) of total pDNA content in the nanogel formulation was added to each well, as nanogels contain a final loaded pDNA quantity of 52.5 μg/2.5 mL. Upon transfection at a larger scale, 2.5 mL (52.5 μg/2.5 mL) of the nanogel formulation was added to each dish. In both small and large-scale experiments, 72 hours post-transfection, the eGFP expression from the pAAV plasmid was checked under the fluorescence microscope (Evos FL, Thermo Fisher Scientific, UK).

2.7 Small scale vector production without concentration of vector particles

Following small-scale transfections, 500 μL of cell supernatant was collected after 72 hours of incubation with nanogels and PEI-MAX/pDNA formulations. Magnesium chloride ($MgCl_2$) was added to the cell supernatant to a final concentration of 1 mM, subsequently, 150 U mL^{-1} of Benzonase (Sigma, Dorset, UK) was added and the supernatant was incubated at 37 °C for 1 hour. Samples were centrifuged at 4200 rpm for 30 minutes at 15 °C and the viral titer of the supernatant was assessed by quantitative polymerase chain reaction (qPCR) (StepOnePlus Real-Time PCR System, ThermoFisher Scientific, UK).

2.7.1 Larger scale vector production with the concentration of vector particles. The method for purification is detailed in and adapted from Hughes *et al.*[45] After 72 hours of incubation in the 10 dishes, 15–20 mL of cell media supernatant and cells from the dishes were collected and centrifuged (Avanti J-15R Centrifuge, Beckman Coulter, Brea CA, USA), at 2000*g* for 10 minutes and resuspended in lysis buffer (140 mM NaCl, 5 mM KCl, 0.7 mM K_2HPO_4, 3.5 mM $MgCl_2$, 25 mM Tris at pH 7.5). Ammonium sulphate (31.3 g/100 mL) was added to the media supernatant and incubated on ice for 30 minutes. The cells were spun for 30 minutes at 8300*g* and the pellet was resuspended in 5 mL lysis buffer. The pellet was subjected to four freeze–thaw cycles between −80 °C for 30 minutes and 37 °C for 20 minutes with vortexing. A final concentration of 1 mM $MgCl_2$ was added followed by 150 U mL^{-1} of benzonase and incubated at 37 °C for 1 hour before centrifuging at 4200 rpm for 30 minutes at 15 °C to clarify the lysate. Iodixanol (OptiPrep, Sigma Aldrich, UK) gradients were prepared for purification, where concentrations of iodixanol were layered in ultracentrifuge tubes (Beckman Instruments, High Wycombe, UK) starting from the highest concentration of 60% followed by 40%, 25% and 15%. The lysate was added over the final iodixanol layer, and the tubes were centrifuged by ultra-centrifugation (Optima XE Ultracentrifuge, Beckman Instruments, High Wycombe, UK) using an SW32-Ti rotor at 32 000 rpm at 18 °C for 5 hours and 15 minutes. Subsequently, 19-gauge needles were used to aspirate the 40% iodixanol gradient layer, which then underwent dilution in phosphate-buffered saline MK (PBS-MK) (PBS, 1 mM $MgCl_2$, 2.5 mM KCl) and filtration through 0.22 μm filters.

The AAV was concentrated using the Vivaspin 20 centrifugal concentrators with an MWCO of 100 000 (Sartorius, Epsom,

UK). The membrane was incubated with 5 mL of 0.1% Pluronic F68 (Gibco, Massachusetts, USA) for 10 minutes, before being replaced with 5 mL 0.01% Pluronic F68 and centrifuged at 3000 rpm for 5 minutes at 4 °C. The filtrate was discarded and the membrane was filled with 5 mL of 0.001% Pluronic F68 with 200 mM NaCl PBS and centrifuged at 3000 rpm for 5 minutes at 4 °C. The viral titer of the concentrated AAV was assessed by qPCR using primers to the ITR sequence.

2.8 Nanogel and polyplex characterisation

Particle characterisation including size, polydispersity index (PDI), zeta potential measurements and particle concentration was carried out using dynamic light scattering (ZetaSizer Ultra, Malvern Panalytical, UK). The measurement temperature was maintained at 25 °C for all readings. For the zeta potential, samples were placed in DTS1070 folded capillary zeta cells (Malvern Panalytical, UK). Nanogels and PEI-MAX/pDNA polyplexes were also assessed using transmission electron microscopy (TEM). Samples were diluted 1 in 5 and placed on copper grids coated with a carbon support film. TEM analysis took place using a Phillips/FEI CM120 Bio Twin Transmission Electron Microscope (Oregon, USA).

2.9 MTT assay

The CellTiter 96 non-radioactive cell proliferation assay MTT kit (Promega, UK) was used to test the cell viability of the nanogels and PEI-MAX polyplexes. HEK293T cells were seeded at a density of 0.1×10^5 cells per well in a 96-well plate. Following 24 hours of incubation, cells were transfected as per section 2.7.1 and incubated for 72 hours in total. Untreated cells were used as a positive control and media alone was used as the negative control. Post-transfection, all media was removed from the well and 15 μL of dye and 100 μL of cell media were added to the wells and incubated for 4 hours. After this time, 100 μL of stop solution was added to each well and incubated at 4 °C for up to 24 hours before measuring absorbance at 570 nm using a SpectraMax Microplate reader (Molecular Devices, Wokingham, UK). Cell viability was determined by the following equation:

$$\%\,\text{Cell Viability} = \frac{(\text{treated cells} - \text{negative control})}{(\text{positve control} - \text{negative control})} \times 100$$

3 Results and discussion

3.1 Nanogel production and particle characterisation

3.1.1 Nanogels and PEI-MAX polyplexes with pDNA weight ratio of 1 : 1 : 3. Nanogels were produced in the CFR at varying NP ratios in order to assess the most suitable for triple transfection, in terms of their particle characteristics and ultimately viral genome production. It is widely reported that with a rising NP ratio, higher levels of transfection are achieved due to charge-facilitated cellular entry, often at the expense of cell viability in many systems.[46] Analysing the optimum NP ratio requires investigating a number of key physicochemical properties for transfection, including particle size, PDI, zeta potential and particle concentration. Particle sizes of 200 nm or below were targeted in this work, given that common endocytic pathways for nanoparticles are generally facilitated below this size,[47] thus increasing the potential for transfection. Successful nanogel and polyplex production would also include particles with a PDI below 0.3, indicating a high degree of monodispersity, whilst a zeta potential in the cationic range would generally be desirable for enhancing cellular entry and determining transfection.[46]

Nanogels and PEI-MAX/pDNA polyplexes were initially prepared at a weight ratio of 1 : 1 : 3 of pAAV, pDG9 and PHGTI respectively, using NP ratios of 10, 15, 20 and 25. The size of particles prepared using the 1 : 1 : 3 weight ratio, are all below 200 nm based on three independently produced batches (Fig. 3a). PEI-MAX/pDNA polyplexes show an average particle size of 152.4 ± 16.4 nm, where particle sizes for nanogels ranged from 127.1 ± 8.2 nm at NP20 to 167.0 ± 22.3 nm at NP25. All nanogels showed no significant difference in the size displayed by PEI-MAX/pDNA polyplexes (P = 0.486, 0.360, 0.370 and 0.881 for NP10, 15, 20 and 25 respectively).

The zeta potential of the particles is a fundamental component of nanoparticle characterisation. Positively charged particles are often able to transfect cells with greater ease, given the ionic attraction to the oppositely charged cell membrane.[17,48] The zeta potential of the PEI-MAX polyplexes with a 1 : 1 : 3 ratio of pDNA shows positively charged particles with a value of 12.4 ± 1.5 mV (Fig. 3b). The nanogels have an overall net negative charge, which is likely attributed to the two negatively charged entities in the formulation; sodium tripolyphosphate and pDNA. The small rise in zeta potential from −28.4 ± 0.4 mV at NP10 to −23.2 ± 0.5 mV at NP25 can be attributed to the increasing quantity of cationic polymer as the NP ratio increases. It is acknowledged that whilst cationic surface charges are generally consistent with successful transfection, various other characteristics must be considered, not least that particles may enter the cell by means other than electrostatic interaction at the cell surface. Therefore, at this stage, it is reasonable not to rule out the possibility of nanogels with weak negative surface charges transfecting cells, which is further explored in section 3.2.

The PDI is a measure of the degree of monodispersity between the particles, where values of 0.3 or below indicate a high level of monodispersity[49] within the nanogels, hence decreasing the size distribution around the mean. Microfluidic production allows for both rapid and homogenous mixing of solutions resulting in low PDI values compared to bulk-mixing methods,[50] and was employed in this study to produce monodisperse nanogels with the potential for continuous production. Fig. 3(c) reveals that increasing NP ratios of the nanogels results in a decrease in the PDI, achieving values as low as 0.070 ± 0.016 at NP25, indicating highly monodisperse particles can be produced in the CFR. The PDI of nanogels at NP20 and NP25 was statistically lower (P = 0.040 and 0.010 respectively) than the PDI of PEI-MAX/pDNA polyplexes. Whilst no minimum particle concentration was determined before

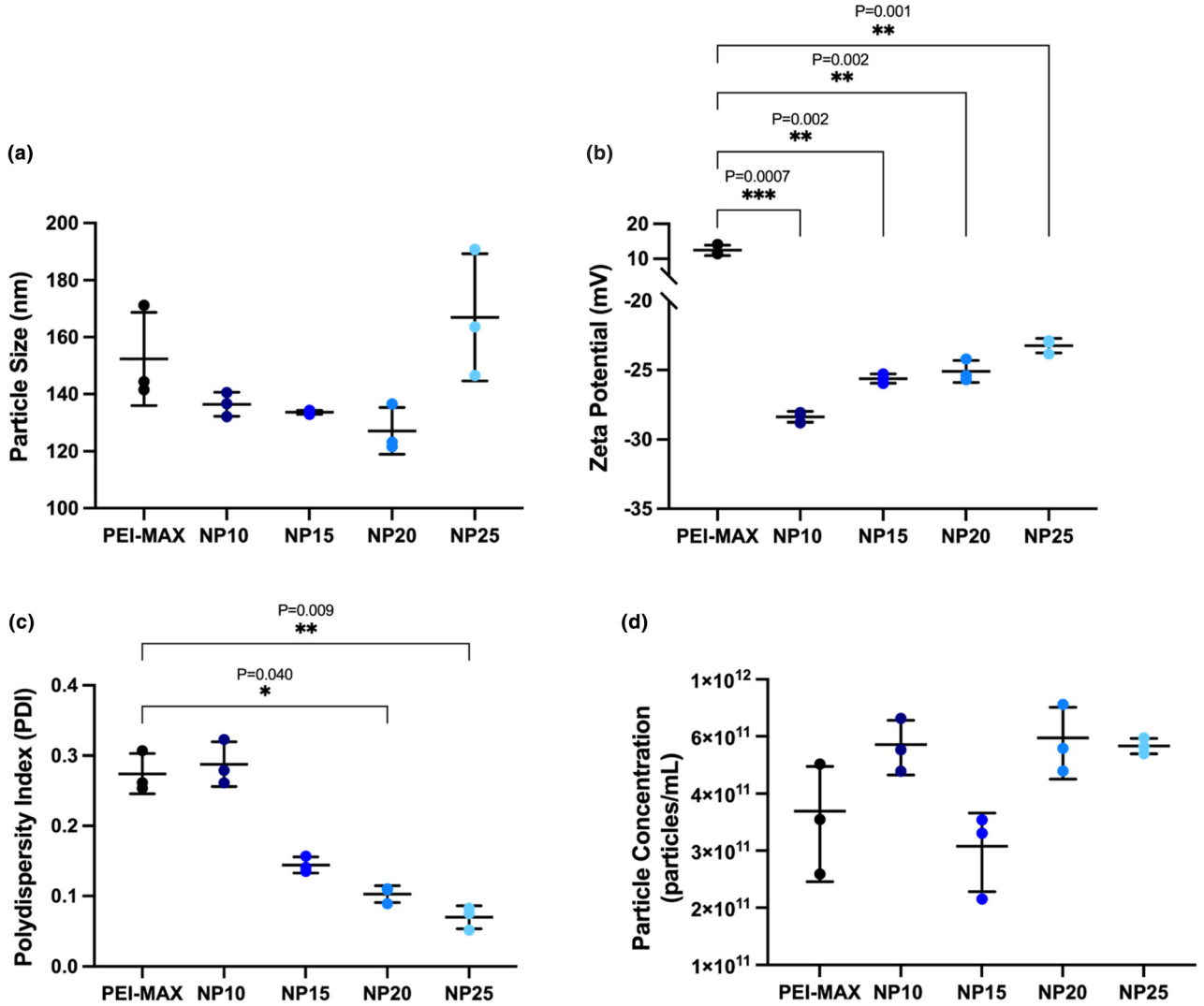

Fig. 3 Particle characterisation comparing increasing NP ratios of nanogels (10, 15, 20, 25) produced by microfluidics, to the control PEI-MAX/pDNA polyplexes produced in standard batch production. All data depict the pDNA weight ratio of 1 : 1 : 3 for pAAV, pDG9 and pHGTI respectively, where each graph demonstrates; (a) particle size (nm), (b) zeta potential (mV) (c) PDI (d) particle concentration (particles per mL). Data are represented as individual points with mean ± standard deviation and a one-way ANOVA study and Dunnett's multiple comparison test were conducted, comparing the mean of each nanogel formulation to the control group PEI-MAX.

the study, the parameter was measured to ensure microfluidics could yield a similar or higher particle concentration to that of PEI-MAX production. Particle concentration of the nanogels showed no significant difference from that of PEI-MAX/pDNA particles, where values ranged between 2.60×10^{11} particles per mL ± 7.70×10^{10} and 6.23×10^{11} particles per mL ± 1.75×10^{11}, as shown in Fig. 3(d).

Nanogels and polyplexes produced at NP ratios from 10–25 displayed mean sizes below the desired 200 nm and below 0.3 PDI, which were used as criteria for predicting successful transfection. The negative zeta potential observed may impede the ability of the formulation to be endocytosed upon transfection. Although negative surface charges are not desirable, the nanogel characteristics of size and PDI assessed in this section, are useful indicators of positive transfection and consequently high viral titres. Therefore, section 3.2 explores the viral titer produced from nanogels at varying NP ratios to ascertain the relationship between titer concentration and particle characteristics.

3.1.2 Nanogels and PEI-MAX polyplexes with pDNA weight ratios of 1 : 1 : 2. Nanogels and PEI-MAX/pDNA polyplexes were also produced at pDNA weight ratios of 1 : 1 : 2 of pAAV, pDG9 and PHGTI respectively, where the total quantity of pDNA remained the same as for the 1 : 1 : 3 weight ratio. PEI-MAX/pDNA nanoparticles with a pDNA ratio of 1 : 1 : 2 had an average particle size of 224.4 ± 21.1 nm, statistically higher (p = 0.0095) than PEI-MAX/pDNA particles at 1 : 1 : 3 ratio of size 152.4 ± 16.4 nm (Fig. 4a). The smaller size of the particles produced at 1 : 1 : 2 may be due to the presence of a lower quantity of the pHelper plasmid, which has a large size of 17.8 kb in

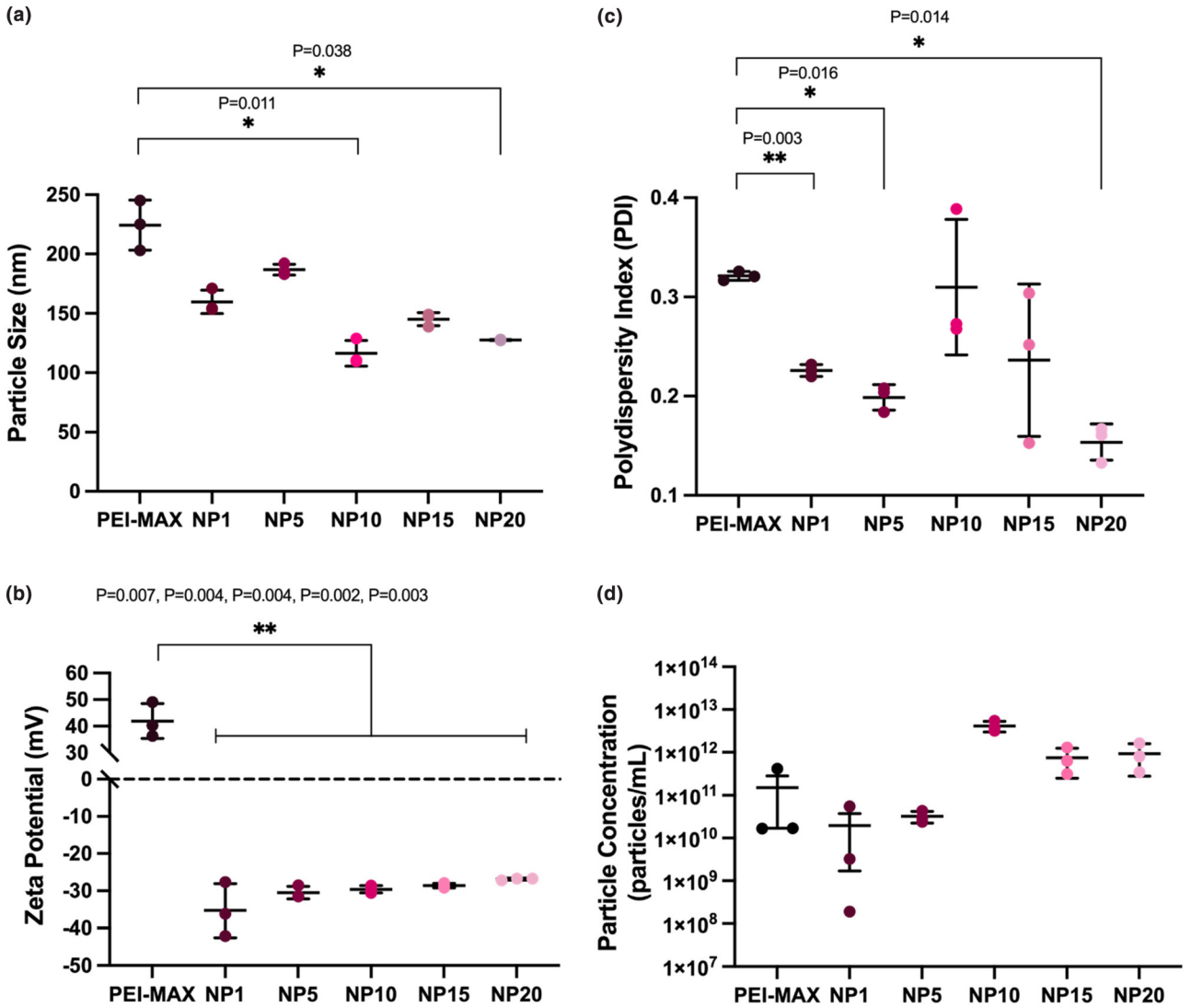

Fig. 4 Particle characterisation results comparing increasing NP ratios of nanogels (1, 5, 10, 15, 20) produced by microfluidics, to the control PEI-MAX/pDNA polyplexes produced in standard batch production. All data depict the pDNA weight ratio of 1 : 1 : 2 for pAAV, pDG9 and pHGTI respectively, where each graph demonstrates; (a) particle size (nm), (b) zeta potential (mV) (c) PDI (d) particle concentration (particles per mL). Data are represented as individual data points and the mean ± standard deviation and a one-way ANOVA study and Dunnett's multiple comparison test were conducted.

comparison to 6.2 kb and 7.9 kb for pAAV and pDG9 respectively. As the pHelper is approximately 2.5 to 3 times larger than the other plasmids, this could contribute to increases in particle size.

The overall charge balance of the particles remained equivalent between the two weight ratios used, therefore the zeta potential of the nanogels showed no significant differences between weight ratios. The zeta potential of the particles produced with 1 : 1 : 2 ratios range from −35.3 mV ± 7.3 at NP1 to −26.9 mV ± 0.3 at NP20 (Fig. 4b), mimicking the correlation in Fig. 3(b) where increasing NP ratios led to increasingly positive surface charge values. PEI-MAX/pDNA particles at 1 : 1 : 2 ratios had a zeta potential of 41.9 ± 6.6 mV, a significantly higher (p = 0.0016) surface charge than the particles produced at 1 : 1 : 3 ratios. We would not anticipate a difference between the two samples, as the overall charges present in the particle remain the same, hence any differences may highlight the inconsistency in the production and physicochemical properties of PEI-MAX/pDNA polyplexes from different batches.

A high degree of polydispersity is demonstrated in the PEI-MAX/pDNA particles produced at 1 : 1 : 2 ratios, as the value of 0.321 ± 0.004 is greater than the recommended value of <0.3.[49] The PDI of nanogel samples ranged from 0.154 ± 0.018 at NP20 to 0.310 ± 0.068 at NP10, where again the lowest PDI value was seen at the highest NP ratio. The particle concentration ranged from 1.96 × 10^{10} particles per mL ± 3.10 × 10^{10} at NP1 to 4.13 × 10^{12} particles per mL ± 1.16 × 10^{12} at NP10, which may be explained by the particle size displaying the smallest size at NP10, indicating that a higher number of smaller particles are forming. Thus, as per the nanogels pro-

duced at 1 : 1 : 3 ratios, nanogels at 1 : 1 : 2 largely met the success criteria of size, PDI and particle concentration.

3.2 Small-scale AAV production

Initial assessments of AAV viral vector production from PEI-MAX/pDNA polyplexes and nanogels were performed at a small scale in 6-well plates of HEK293T cells. At 72 hours post-transfection of PEI-MAX/pDNA and nanogels, the GFP expression from the cells was observed to confirm the release of the plasmids from the nanogel complexes and thus successful transfection, followed by the assessment of the cell supernatant for AAV titer production. Fig. 5(a) and (g) demonstrate the positive control of PEI-MAX/pDNA at 1 : 1 : 2 and 1 : 1 : 3 ratios respectively, where high levels of GFP expression can be seen 72 hours post-transfection. As expected, the negative controls (Fig. 5(b and h) show no GFP expression as the three plasmids were not complexed with a transfection reagent. Although GFP expression was observed with all nanogel formulations (Fig. 5c–f and i–l), reveal that higher levels of expression appear to be at higher NP ratios, which may be rationalised by the higher concentration of CMC–bPEI polymer with increasing NP ratio. In this study, increasing the polymer content of the formulation increases the molar concentration of nitrogen, responsible for producing a more positive surface charge of the particles, theoretically leading to higher levels of transfection.[46]

The viral genomes produced per mL (vg mL^{-1}) were assessed by measuring their presence in the supernatant of the cells 72 hours post-transfection using qPCR. As can be seen in Fig. 6(a) and (b), which show the viral titer for pDNA ratios of 1 : 1 : 3 and 1 : 1 : 2 respectively, higher NP ratios led to lower titer production. Nanogels at NP10 with a 1 : 1 : 3 weight ratio produced a viral titer of 2.07×10^8 vg $mL^{-1} \pm 1.85 \times 10^8$, which presented no significant difference ($P = 0.5817$) to the titer of 5.63×10^8 vg $mL^{-1} \pm 3.39 \times 10^8$, produced by PEI-MAX/pDNA polyplexes. Nanogels formed at higher NP ratios of NP15, 20 and 25 all showed AAV titers which were significantly lower than PEI-MAX ($P = 0.0396$, 0.0404 and 0.0369 respectively). Nanogels with 1 : 1 : 2 weight ratios were produced with NP ratios ranging from 1–20, rather than 5–25 as seen with 1 : 1 : 3 weight ratios, due to the previous success of lower NP ratios of nanogels as seen in Fig. 6a. For 1 : 1 : 2 weight ratios, it was found that NP5 and NP10 nanogels at 8.83×10^8 vg $mL^{-1} \pm 9.71 \times 10^7$ and 8.13×10^8 vg $mL^{-1} \pm 4.97 \times 10^8$ were statistically equivalent in titer to PEI-MAX at 1.09×10^9 vg $mL^{-1} \pm 5.44 \times 10^8$ ($P = 0.866$ and 0.7003 respectively). The nanogels demonstrated equivalent titres to the commercially available transfection agents in spite of the negative surface

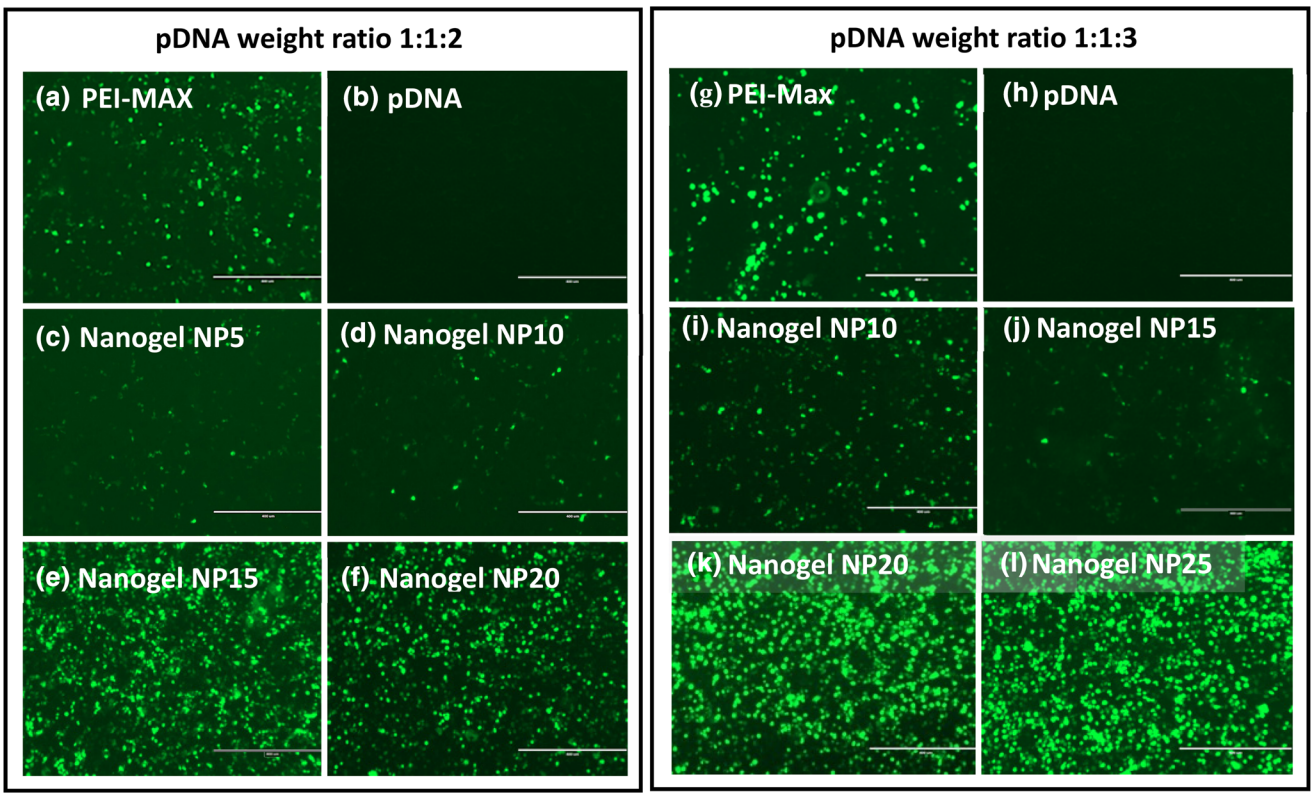

Fig. 5 Fluorescence microscopy images of GFP expression in HEK293T cells 72 hours post-transfection, (a–f) represents PEI-MAX/pDNA nanoparticles and nanogels at 1 : 1 : 2 pDNA weight ratios and (g–l) represents pDNA weight ratios of 1 : 1 : 3. Individual images show; (a) PEI-MAX/pDNA nanoparticles, (b) HEK293T cells transfected with pDNA in the absence of vector, (c–f) nanogels at NP ratios from NP5–20 respectively, (g) PEI-MAX/pDNA nanoparticles, (h) HEK293T cells transfected with pDNA in the absence of vector, (i–l) nanogels at NP ratios from NP10–25 respectively. Scale bars: 400 μm.

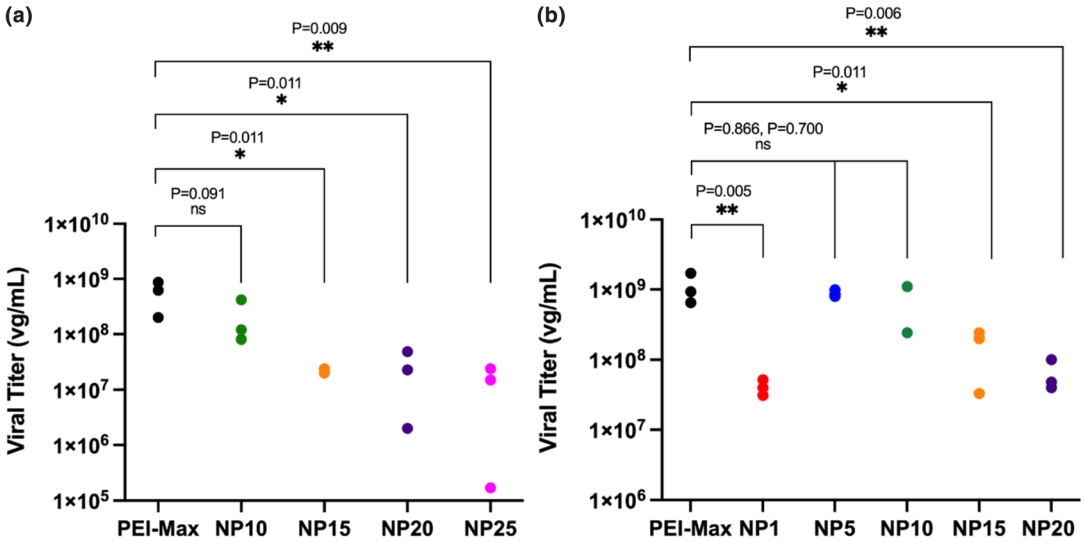

Fig. 6 AAV viral titer from small-scale 6-well plate transfections, where (a) represents pDNA weight ratios of 1 : 1 : 3 and (b) represents pDNA weight ratios of 1 : 1 : 2. One-way ANOVA.

charge previously discussed in section 3.1, which would indicate that the surface charge does not impede the transfection of nanogels and subsequently the viral titre. Interestingly, further decreases in the NP ratio to NP1 resulted in a reduction in viral titer to 4.10×10^7 vg $mL^{-1} \pm 1.05 \times 10^7$, significantly lower ($P$ = 0.0051) than PEI-MAX. At NP ratios below 5, the polymer concentration decreases, indicating that there may not be enough polymer to effectively encapsulate the three plasmids. It could therefore be deduced that NP5 and NP10 possess enough polymer to effectively encapsulate the pDNA; however, higher NP ratios may further condense the pDNA as shown in Fig. 7, hindering the release of the cargo from the polymer.

The data in Fig. 6 contrasts with the findings from the initial transfection experiments in Fig. 5, where the latter indicates that increasing the NP ratio of the nanogels increases the level of GFP expression and hence transfection. Conversely, the data in Fig. 6 indicates that increasing the NP ratio decreases the viral titer produced. A possible explanation for this may be that the GFP expression displayed in Fig. 5 only signifies transfection of one of the three plasmids, the *cis*-plasmid pAAV, which is the only one of the three to contain the GFP expression gene. As previously discussed, pHelper is around 3 times larger than the pAAV and pDG9 plasmids, indicating that the release of this larger structure from the polymer may be hindered *in vitro* compared to the smaller plasmids. Successful AAV production relies on the release of all three plasmids in the triple transfection process, hence delays in the release of one or more of the plasmids would inhibit AAV formation.

3.2.1 Assessment of the physical interactions between particles, nanogels and plasmid DNA using transmission electron microscopy (TEM). TEM imaging was performed on the PEI-MAX/pDNA polyplexes, NP10 and NP20 nanogels at a 1 : 1 : 2 weight ratio to observe the size, shape and morphology of the particles and nanogels. Following sample preparation,

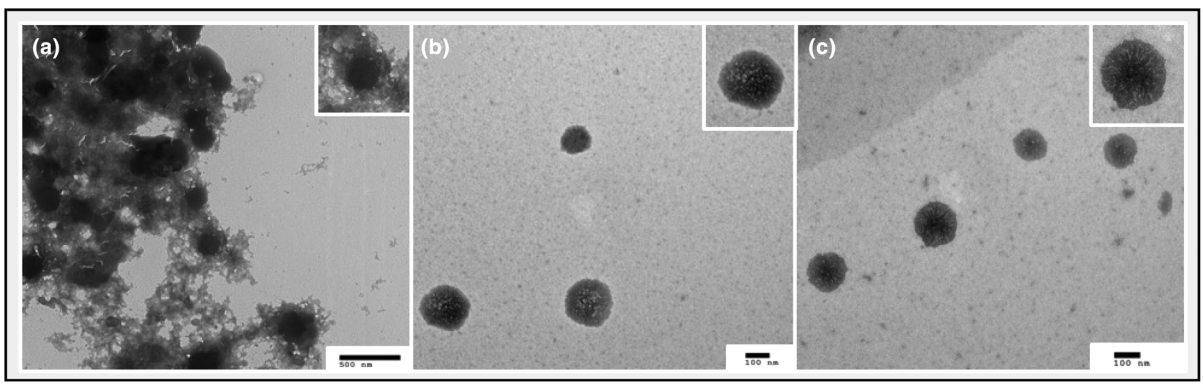

Fig. 7 Transmission Electron Microscopy (TEM) images (a) PEI-MAX/pDNA polyplexes at 1 : 1 : 2 pDNA ratio. Scale bar = 500 nm (b) NP10 nanogels at 1 : 1 : 2 pDNA ratio where the scale = 100 nm and (c) NP20 nanogels at 1 : 1 : 2 weight ratio where the scale bar = 100 nm.

the particles were assessed within 30 minutes and the images were collected. PEI-MAX/pDNA polyplexes formed aggregates, likely owing to the excess PEI-MAX polymer solution, which over time could lead to the instability of PEI-MAX formulations (Fig. 7a). NP10 and NP20 nanogels produced highly dispersed particles that lacked aggregation (Fig. 7b and c). Of note, the nanogels at NP10 appear to have a slightly more porous structure in comparison to NP20 nanogels, with a dense core appearance. This may be a result of the higher polymer content of NP20 nanogels, causing the pDNA to condense in the core of the particle. With rising polymer concentration, there is a higher cationic charge present, allowing greater opportunity to attract and condense the anionic pDNA. Previous triple transfections in Fig. 6 indicated that for both 1 : 1 : 2 and 1 : 1 : 3 weight ratios of pDNA, higher NP ratios resulted in lower viral titers, hence the condensed structure of NP20 nanogels may be critical in impeding pDNA release *in vitro*. The TEM images in Fig. 7 display a high degree of contrast due to the high polymer content of both the PEI-Max nanoparticles and the nanogels. This aids in highlighting the clear distinction between the aggregates in Fig. 7a and the dispersed, more stable particles in Fig. 7b and c.

3.3 Large-scale AAV production

Promising results in small-scale production of AAV without concentration indicated that nanogels produced with NP ratios of 5 and 10 (1 : 1 : 2) and NP10 (1 : 1 : 3) could produce AAV at equivalent titers to PEI-MAX. Therefore, we aimed to evaluate if this was also the case in larger AAV production scale and following concentration of viral particles. Viral titers produced from nanogels were generally higher at all NP ratios using the 1 : 1 : 2 weight ratio, in conjunction with the lower variation around the mean titer, indicating reduced batch-to-batch differences. Nanogels with 1 : 1 : 2 ratios were subjected to an MTT assay (Fig. 8a), where the cell death of HEK293T cells was evaluated and compared to the cell viability of PEI-MAX. Nanogels at the lowest NP ratios of NP1 and NP5 demonstrated cell viabilities of 101.0% ± 2.0 and 93.5% ± 2.9 respectively. The lower concentration of polymer used in both formulations may be the cause of the lower cell viability as it is well-researched that the high cationic nature of PEI can lead to significant cell death. PEI-MAX shows cell viability of 44.5% ± 15.1, comparable to the nanogel formulation at both NP10 and NP20. For this reason, given that nanogels produced at NP5 and NP10 produce equivalent viral titers, an NP ratio of 5 was selected for AAV production at large scale, due to its lower tendency to cause cell death. It is of note that the particle characteristics for the NP5 nanogels used for large-scale AAV manufacture are the same as those reported for small-scale manufacture and have therefore been reported previously in section 3.1.2.

As shown in Fig. 8b, the titer of the concentrated AAV9 vector produced from nanogels at NP5 and PEI-MAX, showed no statistically significant difference, revealing viral titers of 7.41×10^{11} vg mL^{-1} ± 1.36×10^{11} and 1.24×10^{12} vg mL^{-1} ± 4.4×10^{11} respectively. It is, therefore, possible to denote that alternative methods of producing AAV viral vectors are available, whereby equivalent titers can be achieved. The work demonstrates that AAV production is attainable at lower costs compared to PEI-MAX and by continuous production, ensuring that batch-to-batch variation and disparities in operator skill levels can be alleviated. The coaxial flow reactor, therefore, has the potential to provide a cost-effective, reproducible and scalable approach to the manufacture of nanogels for triple transfection.

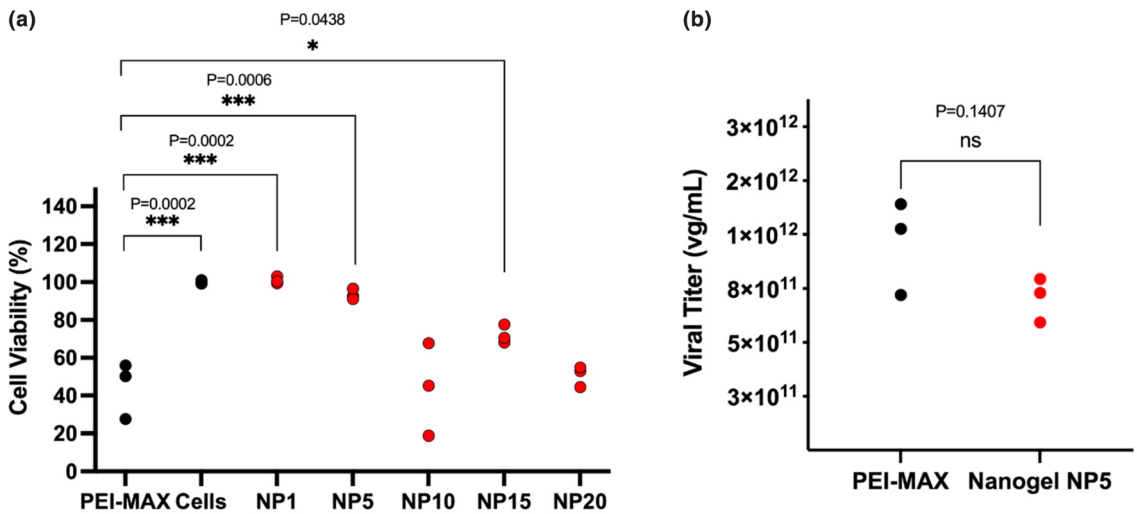

Fig. 8 (a) MTT assay to assess the cell viability of PEI-MAX and nanogels at NP1–NP20 on HEK293T cells, 72 hours post-transfection. Cell viability (%) is expressed as a percentage of the untreated control cells where data are represented as individual points. A one-way ANOVA study and Dunnett's multiple comparison test were performed to compare nanogels at various NP ratios with the positive control group of PEI-MAX/pDNA polyplexes. (b) AAV viral titer production at a large scale, comparing the titer production with PEI-MAX and the optimised nanogels at NP5 using a pDNA weight ratio of 1 : 1 : 2, with vg mL^{-1} referring to viral genomes per mL. A two-tailed unpaired *t*-test was conducted comparing the mean titers of the two groups where data are presented as individual points.

4 Conclusions

AAV vectors have seen unprecedented success in the clinic in recent years, achieved in parallel to an increased demand for improved and reproducible manufacturing techniques suitable for supporting this growth. Current production methods remain unsatisfactory for meeting manufacturing needs, hence means of producing vectors in quantities required for late-stage development in academic and clinical settings alike are highly sought after.[51]

In this study, a microfluidic platform for the production of nanogels encapsulating pDNA was used in the triple transfection process, as an alternative to current production systems such as PEI-MAX/pDNA particles. Microfluidics confers many benefits over typical batch production systems, as continuous production can be achieved, allowing operators to reliably and uniformly manufacture formulations for each transfection. Nanogels were initially prepared by varying the pDNA weight ratios of the three plasmids at 1 : 1 : 2 and 1 : 1 : 3. The size, PDI, zeta potential, particle concentration and viral titers were compared to that of PEI-MAX/pDNA polyplexes, typically used for triple transfection of HEK cells.[20,21,26,52–54] Nanogels with both 1 : 1 : 3 and 1 : 1 : 2 pDNA ratios produced particles below 200 nm, necessary for efficient endocytosis. Similarly, nanogels were all largely below a mean PDI value of 0.3, indicating a high degree of monodispersity and an increased likelihood of particles remaining within the desired size range. Despite the expectation that the negative charge of all nanogels produced in this study may impact the transfection efficiency, the AAV vectors produced at a small scale with lower NP ratios successfully transfected HEK293T cells to produce AAV titers equivalent to the control. Nanogels with 1 : 1 : 3 ratios produced viral titers of 2.07×10^8 vg $mL^{-1} \pm 1.85 \times 10^8$ at NP10, showing no significant difference in the titer of PEI-MAX polyplexes at 5.63×10^8 vg $mL^{-1} \pm 3.39 \times 10^8$. Viral titers produced with 1 : 1 : 2 particles were also analogous, where NP5 and NP10 produced 8.83×10^8 vg $mL^{-1} \pm 9.71 \times 10^7$ and 8.13×10^8 vg $mL^{-1} \pm 4.97 \times 10^8$ respectively, statistically equivalent in titer to PEI-MAX at 1.09×10^9 vg $mL^{-1} \pm 5.44 \times 10^8$.

Owing to their overall higher viral titers compared to 1 : 1 : 3 ratios and reduced variation around the mean titer, nanogels at 1 : 1 : 2 ratios were further pursued in large-scale production. A nitrogen/phosphate ratio of 5 demonstrated higher cell viability of 93.5% ± 2.9 compared to 43.9% ± 24.5 at NP10, and for this reason, were chosen for the large-scale viral titer assessment. Production of AAV at this scale revealed that nanogels and PEI-MAX produced equivalent viral titers of 7.41×10^{11} vg $mL^{-1} \pm 1.36 \times 10^{11}$ and 1.24×10^{12} vg $mL^{-1} \pm 4.4 \times 10^{11}$ respectively, indicating that alternative transfection reagents to the classic PEI-MAX are available to synthesise in-house, with the capacity to produce AAV9 in proportionate yields. The results obtained in these experiments were based on one production of AAV, hence multiple experiments run in parallel may be required to evaluate if the nanogel can outperform PEI.

In conclusion, we have demonstrated microfluidic coaxial flow reactors can efficiently produce nanogels for triple transfection with desired viral titers and particle characteristics. The nanogels produced in this work are not bound by the same restrictions as PEI-MAX, where fabrication is not time-limited, costs are comparably lower and the issues surrounding batch-to-batch variation can be circumvented. Microfluidics has been previously implemented in various gene delivery studies, though here we have demonstrated the production of a novel transfection reagent designed for triple transfection, using microfluidic CFR reactors as a means to add control to the synthesis. This study presents the first known use of nanogels as reagents for triple transfection where high AAV titers, equivalent to those of commonly used reagents, are achieved through simple and cost-effective fabrication methods.

Conflicts of interest

No conflicts of interest to declare.

Acknowledgements

This work was supported by the EPSRC [EP\R513143/1] studentship awarded to ZW. We would also like to thank Dr Andrew Weston for the TEM imaging in this study.

References

1 M. Agbandje-McKenna and J. Kleinschmidt, in *Adeno-Associated Virus Methods and Protocols*, 2011, vol. 807, pp. 47–92.
2 Spark Therapeutics, Full Prescribing Information Indictaions and Usage Luxturna (voretigene neparvovec-rzyl) is an adeno-associated virus vector-based gene therapy indicated for the treatment of patients with confirmed biallelic RPE65 mutation-associated retinal dystrophy, 2017.
3 G. A. Rodrigues, E. Shalaev, T. K. Karami, J. Cunningham, N. K. H. Slater and H. M. Rivers, *Pharm. Res.*, 2019, **36**, 1–20.
4 T. T. L. Yu, P. Gupta, V. Ronfard, A. A. Vertès and Y. Bayon, *Front. Bioeng. Biotechnol.*, 2018, **6**, 1–8.
5 D. M. Paton, *Drugs Future*, 2019, **4**, 625–633.
6 D. J. A. Crommelin, R. D. Sindelar and B. Meibohm, *Pharmaceutical biotechnology: Fundamentals and applications*, 2019, pp. 57–82.
7 A. Srivastava, K. M. G. Mallela, N. Deorkar and G. Brophy, *J. Pharm. Sci.*, 2021, **110**, 2609–2624.
8 W. Su, M. I. Patrício, M. R. Duffy, J. M. Krakowiak, L. W. Seymour and R. Cawood, *Nat. Commun.*, 2022, **13**, 1–14.
9 L. Li, E. K. Dimitriadis, Y. Yang, J. Li, Z. Yuan, C. Qiao, C. Beley, R. H. Smith, L. Garcia and R. M. Kotin, *PLoS One*, 2013, **8**, 1–14.
10 R. Carbonell, A. Mukherjee and J. Dordick, *A Technology Roadmap For Today's Gene Therapy Manufacturing Challenges*, https://www.bioprocessonline.com/doc/a-technology-roadmap-

for-today-s-gene-therapy-manufacturing-challenges-0001 (accessed 30 August 2022).
11 M. A. Kotterman and D. V. Schaffer, *Nat. Rev. Genet.*, 2014, **15**, 445–451.
12 T. Kimura, B. Ferran, Y. Tsukahara, Q. Shang, S. Desai, A. Fedoce, D. R. Pimentel, I. Luptak, T. Adachi, Y. Ido, R. Matsui and M. M. Bachschmid, *Sci. Rep.*, 2019, **9**, 1–13.
13 J. C. M. van der Loo and J. F. Wright, *Hum. Mol. Genet.*, 2016, **25**, 42–52.
14 S. E. Reed, E. M. Staley, J. P. Mayginnes, D. J. Pintel and G. E. Tullis, *J. Virol. Methods*, 2006, **138**, 85–98.
15 J. H. Lee and M. J. Welsh, *Gene Ther.*, 1999, **6**, 676–682.
16 J. F. Wright, *Hum. Gene Ther.*, 2009, **20**, 698–706.
17 B. Ma, S. Zhang, H. Jiang, B. Zhao and H. Lv, *J. Controlled Release*, 2007, **123**, 184–194.
18 O. Boussif, F. Lezoualc'h, M. Zanta, M. Mergny, D. Scherman, B. Demeneix and J. Behr, *Biochemistry*, 1995, **92**, 7297–7301.
19 X. Huang, A. V. Hartley, Y. Yin, J. H. Herskowitz, J. J. Lah and K. J. Ressler, *J. Virol. Methods*, 2013, **193**, 270–277.
20 P. D. Trivedi, C. Yu, P. Chaudhuri, E. J. Johnson, T. Caton, L. Adamson, B. J. Byrne, N. K. Paulk and N. Clément, *Mol. Ther. – Methods Clin. Dev.*, 2022, **24**, 154–170.
21 M. Lock, M. Alvira, L. H. Vandenberghe, A. Samanta, J. Toelen, Z. Debyser and J. M. Wilson, *Hum. Gene Ther.*, 2010, **21**, 1259–1271.
22 M. Negrini, G. Wang, A. Heuer, T. Björklund and M. Davidsson, *Curr. Protoc. Neurosci.*, 2020, **93**, 1–10.
23 A. Nyamay'antu, M. Hellal, M. Porte and P. Erbacher, *Cell Gene Ther. Insights*, 2020, **6**, 655–661.
24 P. A. Longo, J. M. Kavran, M.-S. Kim and D. J. Leahy, *Methods Enzymol.*, 2013, **29**, 227–240.
25 A. D. Powers, B. A. Piras, R. K. Clark, T. D. Lockey and M. M. Meagher, *Hum. Gene Ther: Methods.*, 2016, **27**, 112–121.
26 H. Zhao, K. J. Lee, M. Daris, Y. Lin, T. Wolfe, J. Sheng, C. Plewa, S. Wang and W. H. Meisen, *Mol. Ther. – Methods Clin. Dev.*, 2020, **18**, 312–320.
27 B. Strobel, B. Klauser, J. S. Hartig, T. Lamla, F. Gantner and S. Kreuz, *Mol. Ther.*, 2015, **23**, 1582–1591.
28 J. Guan, K. Chen, Y. Si, T. Kim, Z. Zhou, L. Zhou and X. M. Liu, *Front. Chem. Eng.*, 2022, **4**, 1–19.
29 A. V. Kabanov and S. V. Vinogradov, *Angew. Chem., Int. Ed.*, 2009, **48**, 5418–5429.
30 I. Neamtu, A. G. Rusu, A. Diaconu, L. E. Nita and A. P. Chiriac, *Drug Delivery*, 2017, **24**, 539–557.
31 K. McAllister, P. Sazani, M. Adam, M. J. Cho, M. Rubinstein, R. J. Samulski and J. M. DeSimone, *J. Am. Chem. Soc.*, 2002, **124**, 15198–15207.
32 R. Li, W. Wu, H. Song, Y. Ren, M. Yang, J. Li and F. Xu, *Acta Biomater.*, 2016, **41**, 282–292.
33 L. Song, X. Liang, S. Yang, N. Wang, T. He, Y. Wang, L. Zhang, Q. Wu and C. Gong, *Drug Delivery*, 2017, **25**, 122–131.
34 R. Sunasee, P. Wattanaarsakit, M. Ahmed, F. B. Lollmahomed and R. Narain, *Bioconjugate Chem.*, 2012, **23**, 1925–1933.
35 X. Huang, S. Shen, Z. Zhang and J Zhuang, *Int. J. Nanomed.*, 2014, **9**, 4785–4794.
36 A. C. Lima, P. Sher and J. F. Mano, *Expert Opin. Drug Delivery*, 2012, **9**, 231–248.
37 F. S. El-banna, M. E. Mahfouz, S. Leporatti, M. El-Kemary and N. A. N. Hanafy, *Appl. Sci.*, 2019, **9**, 1–11.
38 J. Ahn, J. Ko, S. Lee, J. Yu, Y. T. Kim and N. L. Jeon, *Adv. Drug Delivery Rev.*, 2018, **128**, 29–53.
39 F. S. Majedi, M. M. Hasani-sadrabadi, S. Hojjati, M. A. Shokrgozar, J. J. Vandersarl, E. Dashtimoghadam, A. Bertsch and P. Renaud, *Lab Chip*, 2013, **1**, 204–207.
40 S. Bazban-Shotorbani, E. Dashtimoghadam, A. Karkhaneh, M. M. Hasani-Sadrabadi and K. I. Jacob, *Langmuir*, 2016, **32**, 4996–5003.
41 Z. Whiteley, H. M. K. Ho, Y. X. Gan, L. Panariello, G. Gkogkos, A. Gavriilidis and D. Q. M. Craig, *Nanoscale Adv.*, 2021, **3**, 2039–2055.
42 J. F. Wright, *Gene Ther.*, 2008, **15**, 840–848.
43 S. C. Park, J. P. Nam, Y. M. Kim, J. H. Kim, J. W. Nah and M. K. Jang, *Int. J. Nanomed.*, 2013, **8**, 3663–3677.
44 S. Biswas, T. Ahmed, M. M. Islam, M. S. Islam and M. M. Rahman, *Biomedical applications carboxymethyl chitosans*, INC, 2020, pp. 433–470.
45 M. P. Hughes, D. A. Smith, L. Morris, C. Fletcher, A. Colaco, M. Huebecker, J. Tordo, N. Palomar, G. Massaro, E. Henckaerts, S. N. Waddington, F. M. Platt and A. A. Rahim, *Hum. Mol. Genet.*, 2018, **27**, 3079–3098.
46 Y.-Y. W. Dana, J. Gary, J. B. Min, Y. Kim and K. Park, *Macromol. Biosci.*, 2013, **13**, 1059–1071.
47 J. J. Rennick, A. P. R. Johnston and R. G. Parton, *Nat. Nanotechnol.*, 2021, **16**, 266–276.
48 P. L. Felgner, T. R. Gadek, M. Holm, R. Roman, H. W. Chan, M. Wenz, J. P. Northrop, G. M. Ringold and M. Danielsen, *Proc. Natl. Acad. Sci. U. S. A.*, 1987, **84**, 7413–7417.
49 L. Xu, X. Wang, Y. Liu, G. Yang, R. J. Falconer and C.-X. Zhao, *Adv. NanoBiomed Res.*, 2021, **2100109**, 51–79.
50 M. A. Tomeh and X. Zhao, *Mol. Pharm.*, 2020, **17**, 4421–4434.
51 N. Clément and J. C. Grieger, *Mol. Ther. – Methods Clin. Dev.*, 2016, **3**, 16002.
52 J. C. Grieger, S. M. Soltys and R. J. Samulski, *Mol. Ther.*, 2016, **24**, 287–297.
53 T. N. T. Nguyen, S. Sha, M. S. Hong, A. J. Maloney, P. W. Barone, C. Neufeld, J. Wolfrum, S. L. Springs, A. J. Sinskey and R. D. Braatz, *Mol. Ther. – Methods Clin. Dev.*, 2021, **21**, 642–655.
54 G. K. Chee, X. Kang, Y. Xie, Z. Fei, J. Guan, B. Yu, X. Zhang and L. J. Lee, *Mol. Pharm.*, 2009, **6**, 1333–1342.